Linear Control Systems Project

Milad Heidari

Student ID: 98101469

Course Instructor: M. Babazadeh

1) Introduction

Bicycles are simple vehicles used by many people for transportation, exercise, and recreation. Bicycles are statically unstable, but by proper design, they can be stable in forwarding motion. There are various models with various complexities that are derived by different people over the years. a simple bicycle geometry is illustrated in figure1. In order to describe bicycles' motion, we need a fixed coordinate system that is shown in figure2.

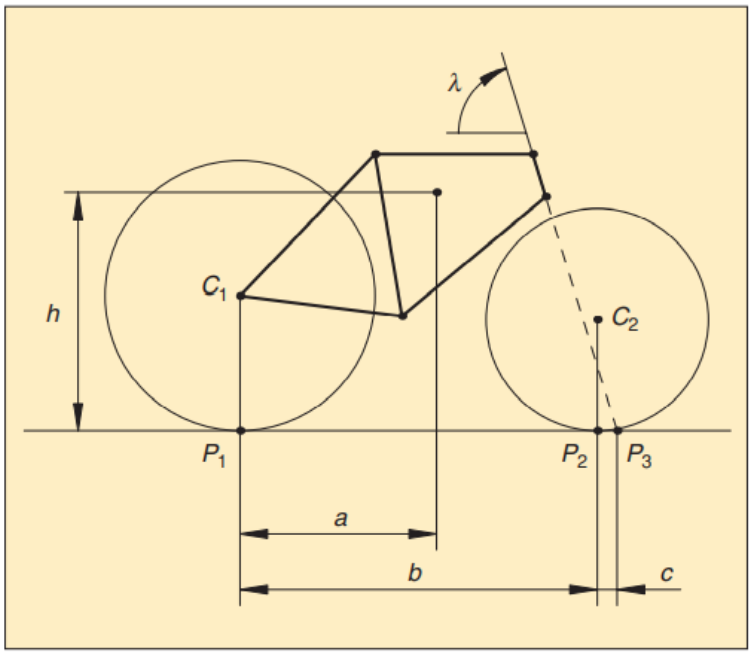

Figure 1. *Parameters defining the bicycle geometry.*

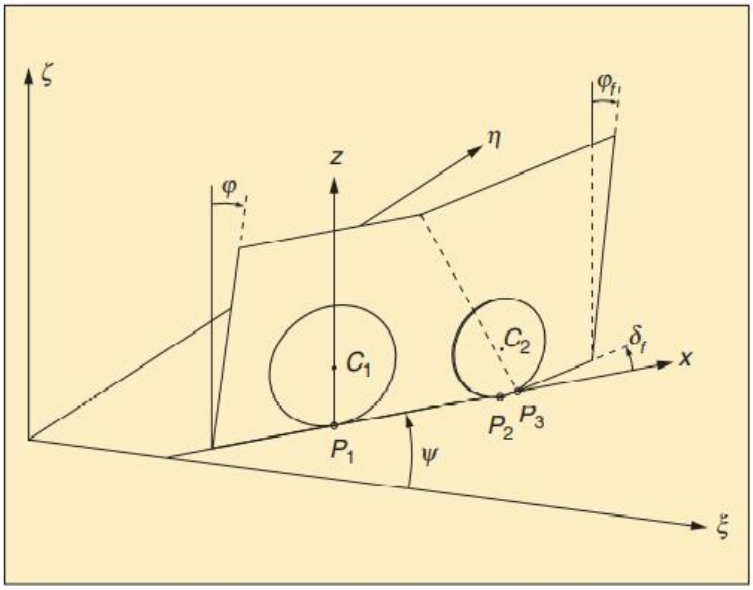

Figure 2. *Coordinate systems. The orthogonal system $\xi\eta\zeta$ is fixed to inertial space, and the ζ-axis is vertical.*

The simplest model is called the **second-order model without a front fork**. This model is unstable and cannot explain why it is possible to ride with no hands. Applying some torque to handlebars creates negative feedback and makes it possible to stabilize this model.

The next model is called **second-order model with a front fork**. The previous model does not capture the effects of the front fork. In this model, we take one step further and define the torque applied to the handlebars as the control variable. The front fork assembly, naturally creates negative feedback and stabilizes the system in the case that velocity is sufficiently large.

The third model to consider is **rear-wheel steering model**. There have been some, however, unsuccessful attempts to develop bicycles having front-wheel drive and rear-wheel steering in the 20th century. Specifically, in the 1970s, the U.S National Highway Safety Administration (NHSA) funded a project aimed at developing a safe rear-wheel steering and front-wheel drive motorcycle. But it turned out to be unrideable because the real part of unstable poles was about 4-12 rad/s which is too fast to be controlled by human riders. It has been concluded that this model is unstable for all positive velocities, no matter what control law is used.

Figure 18. *Klein's original unridable rear-steered bicycle.*

The final and the most complicated model is **linear fourth-order model**. Unlike previous models, this model is obtained using computer software and responds in a much more realistic way to its inputs.

In all the above cases, knowledge of control plays a fundamental role. Using simple models and simulations, we understand the qualitative behavior of bicycles when a torque is applied to handlebars or when rider leans.

Bicycles also exhibit a non-intuitive behavior which is called **non-minimum phase steering behavior**. This phenomenon is explained in detail in the last section. A significant number of motorcycle accidents are caused by riders who fail to counter-steer. Most of the problems associated with zeros in the right-half plane can be eliminated using controllers and actuators.

Finally, with knowledge of bicycle dynamics, rider perceptions, and control, we can design adapted bicycles for children with disabilities. When placing timid children on a bicycle, it is important to provide stability and slower dynamics. This is done by using special wheels called **crowned rollers**.

To wrap up, the bicycle can be used to illustrate a wide variety of control concepts such as modeling, nonlinear dynamics, and codesign of process and control.

2) Stabilization

2.1) Simple Second-Order Model without a Front Fork

In this simple model it is assumed that steer axis is vertical, thus the head angle (λ) is 90°. It also implies that the trail (c) is zero. The control variable is steer angle (δ) and the only degree of freedom is the roll angle (φ).

Writing momentum balance equation and using some approximations for moment of inertia and inertia product, we arrive at the following transfer function from steer angle δ to tilt angle φ:

$$G_{\varphi\delta}(s) = \frac{V(Ds + mVh)}{b(Js^2 - mgh)} = \frac{VD}{bJ}\,\frac{s + \frac{mVh}{D}}{s^2 - \frac{mgh}{J}} \approx \frac{aV}{bh}\,\frac{s + \frac{V}{a}}{s^2 - \frac{g}{h}}$$

The system has two poles at $P_{1,2} = \pm\sqrt{\frac{g}{h}}$ and a zero at $z = -\frac{V}{a}$. It is obvious that the open loop system is unstable for all positive values of V because of the right half-plane pole $\sqrt{\frac{g}{h}}$.

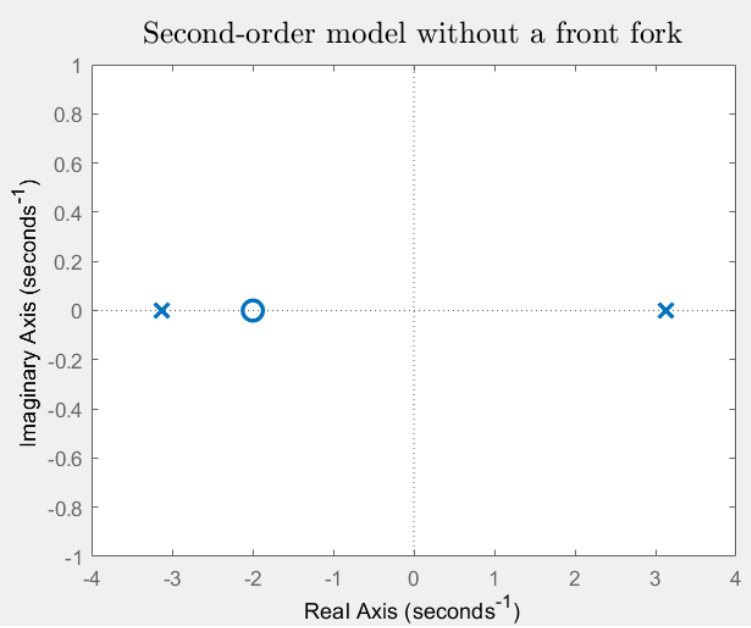

Pole-Zero map of the open-loop system

However, the system can be stabilized using proportional feedback:

$$\delta = -k_2\varphi$$

Which yields the closed-loop system

$$J\frac{d^2\varphi}{dt^2} + \frac{DVk_2}{b}\frac{d\varphi}{dt} + \left(\frac{mV^2hk_2}{b} - mgh\right)\varphi = 0$$

The system characteristic equation is:

$$Js^2 + \frac{DVk_2}{b}s + \left(\frac{mV^2hk_2}{b} - mgh\right) = 0$$

$$mh^2s^2 + \frac{mahVk_2}{b}s + \left(\frac{mV^2hk_2}{b} - mgh\right) = 0$$

If we denote roots of characteristic equation by p_1 and p_2, the general solution for φ is

$$\varphi(t) = Ae^{p_1 t} + Be^{p_2 t}$$

Therefore, the closed loop system is stable if the real parts of p_1 and p_2 are negative.

In the following figure, roots of the characteristic equation are plotted as V (velocity) varies from 0 m/s to 10 m/s and $k_2 = 1$:

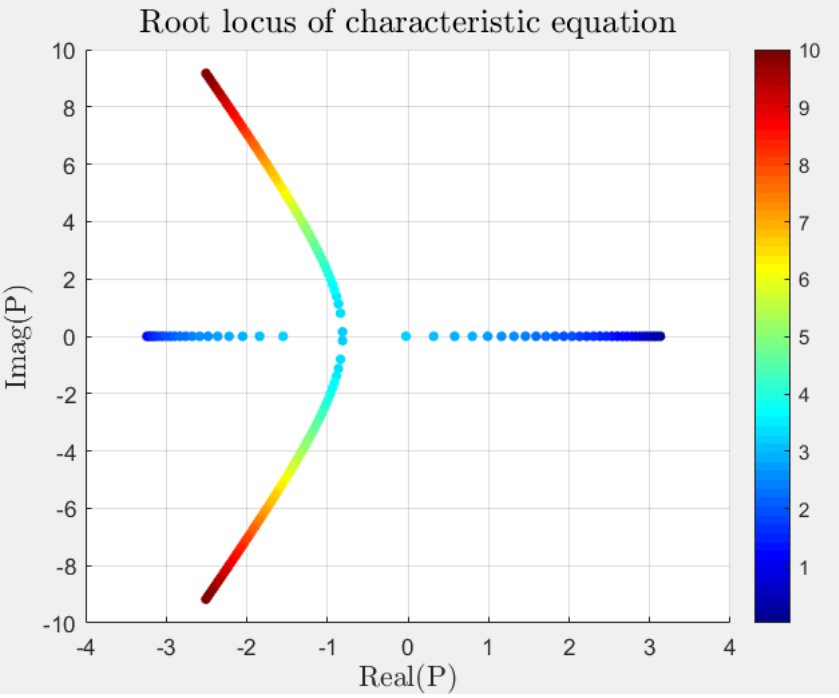

Roots of the characteristic equation of the closed-loop system

The color bar shows the velocity (dark blue dots correspond

to small velocities whereas dark red dots indicate higher velocities)

It can be seen from the graph that the closed-loop system is unstable for low velocities and it becomes stable when the velocity exceeds a threshold. Concretely, this closed-loop system is stable if $k_2 > \frac{bg}{V^2}$ which in the above case it becomes $1 > \frac{9.81}{V^2}$ or $V > \sqrt{9.81} = 3.132$.

2.2) Simple Second-Order Model with a Front Fork

The first model discussed above does not capture the effect of the front fork on bicycle dynamics. To take the front fork into account, unlike the first model we define the torque applied to handlebars (T) as the control variable.

The front fork is simply modeled by a static torque balance. The torque balance for the front fork assembly can be written as

$$\delta = K_1(V)T - K_2(V)\varphi$$

Where $K_1(V)$ and $K_2(V)$ are defined as follows:

$$K_1(V) = \frac{b^2}{(V^2 \sin\lambda - bg\ \cos\lambda)\, mac \sin\lambda}$$

$$K_2(V) = \frac{bg}{V^2 \sin\lambda - bg\ \cos\lambda}$$

It can be seen from equations that by taking the front fork into account, the system provides a negative feedback from tilt angle φ to steering angle δ. Hence, the bicycle can be regarded as a feedback system as illustrated in the following figure:

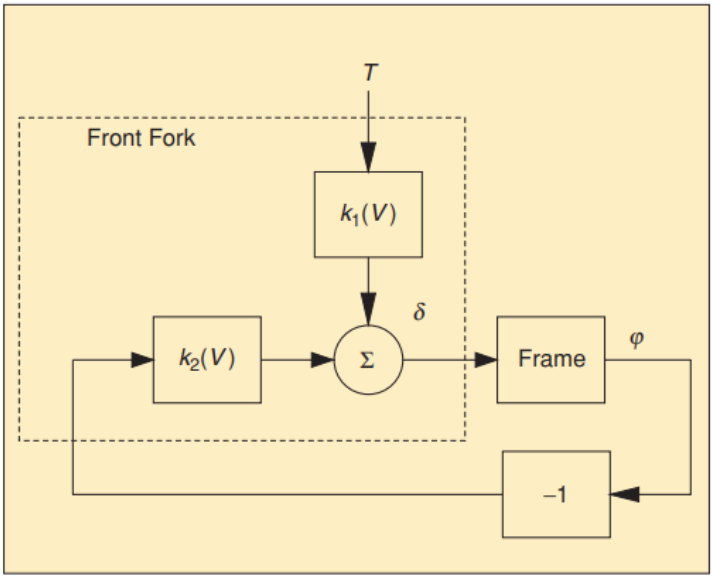

Figure 4. *Block diagram of the bicycle with a front fork. The steer torque applied to the handlebars is T, the roll angle is φ, and the steer angle is δ. Notice that the front fork creates a feedback from the roll angle φ to the steer angle δ, which can stabilize the system.*

By applying angular momentum balance law and noticing the relation between T (torque applied to handlebars) and steer angle δ, we arrive at the following transfer function from torque T to tilt angle φ :

$$G_{\delta T}(s) = \frac{K_1(V)}{1 + K_2(V)G_{\varphi\delta}(s)}$$

where:

$$K_1(V) = \frac{b^2}{(V^2 \sin\lambda - bg\ \cos\lambda)\, mac \sin\lambda}$$

and

$$K_2(V) = \frac{bg}{V^2 \sin\lambda - bg\ \cos\lambda}$$

and

$$G_{\varphi\delta}(s) = \frac{aV}{bh}\ \frac{s + \frac{V}{a}}{s^2 - \frac{g}{h}}$$

Theoretically, the system is stable if the following two conditions hold:

$$V > V_c = \sqrt{bg\ \cot\lambda}$$

and

$$bh > ac\ \tan\lambda$$

To check this statement, we investigate location of poles as V varies in the range $(0, 2V_c)$. Because of the discontinuity in $V = V_c$, it is easier to separate the interval into two sub-intervals $(0, V_c)$ and $(V_c, 2V_c)$.

The following figure illustrates how locations of poles change as V increases from 0 m/s to V_c m/s.

(P_1 and P_2 are poles of the system)

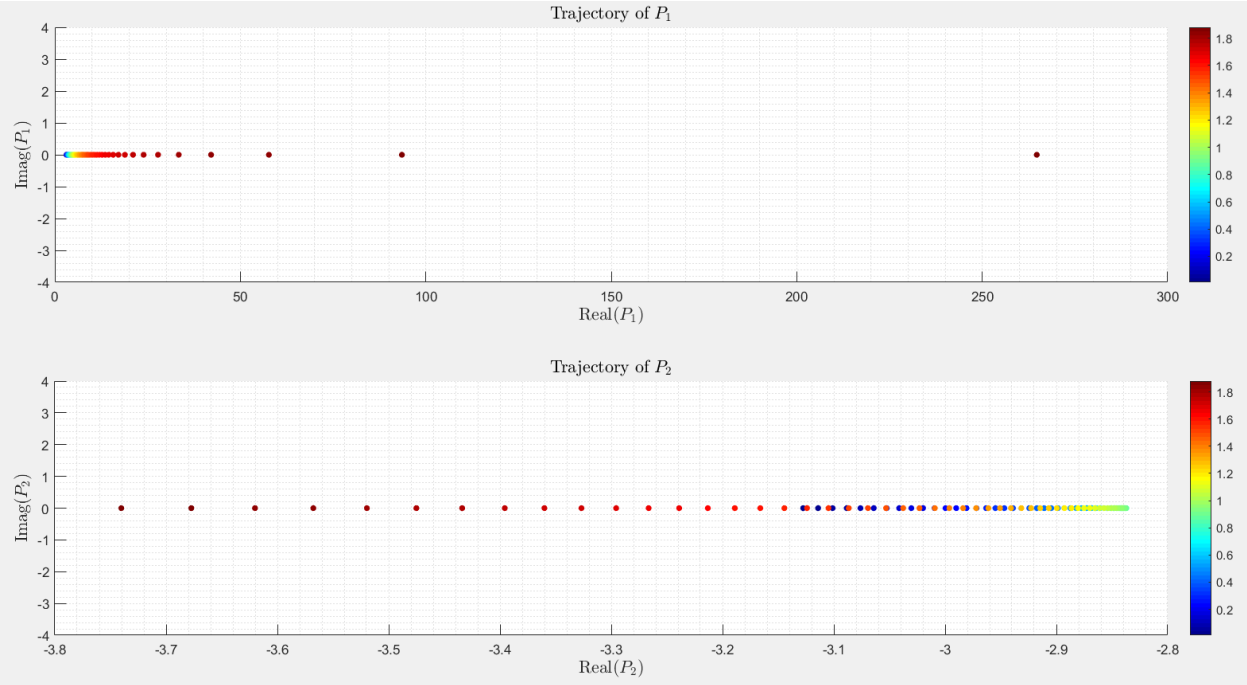

It can be seen that for these values of velocity ($V < V_c$) the system is unstable since one of the poles, namely P_1, lies on the right half plane.

The following figure illustrates how locations of poles change as V increases from V_c m/s to $2V_c$ m/s. (P_1 and P_2 are poles of the system)

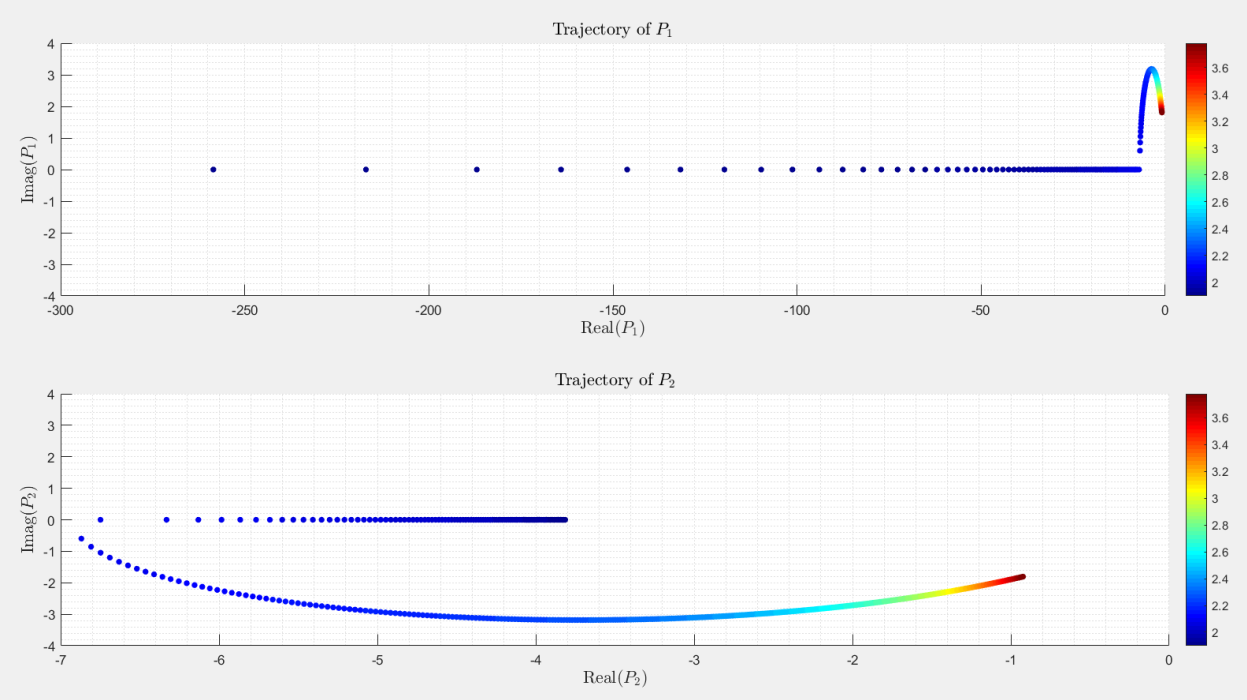

In this case, both poles have negative real part which results in system stability.

An animated graph is also available for this part which dynamically shows the behavior of the poles. Please refer to section5 of the attached “Main.m” script to watch the animation.

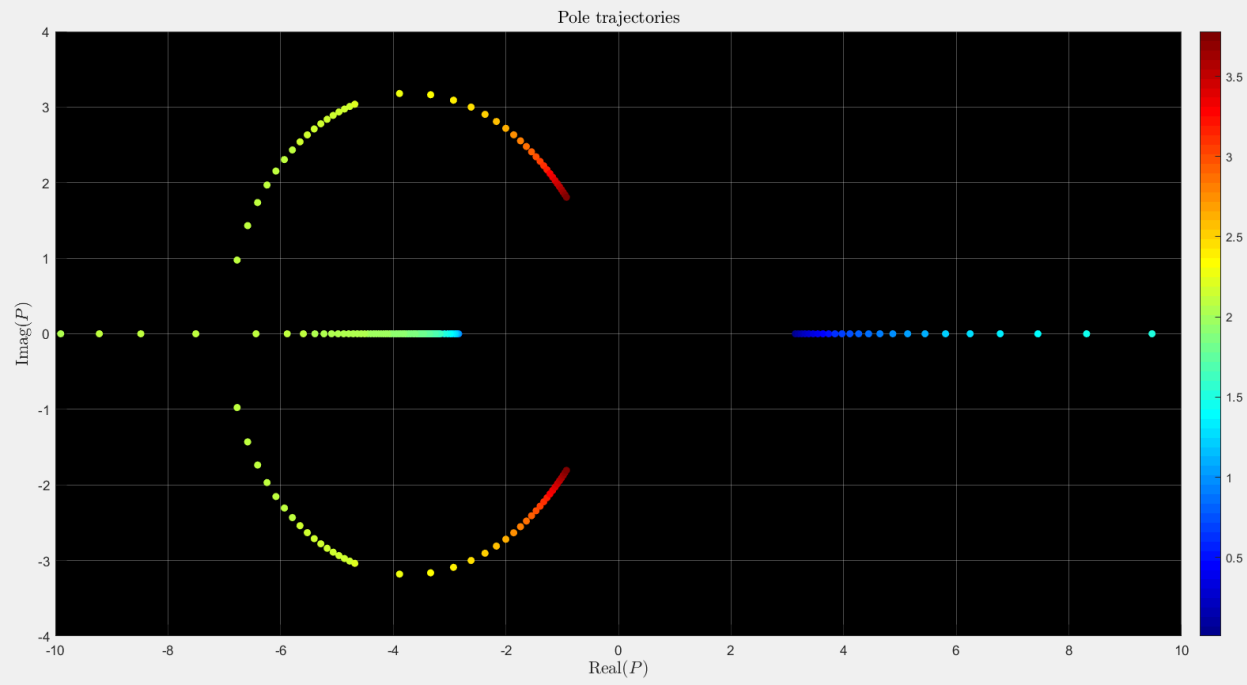

The last frame of the above-mentioned animation. One of the poles initially starts in the right Half plane and moves toward $+\infty$. When critical velocity is reached, both poles appear in the Left half plane and the system becomes stable for velocities greater than critical velocity.

2.3) Bicycle with Rear-Wheel Steering

According to the article, a model for a bicycle with rear-wheel steering is obtained by reversing the sign of the velocity of models with forward-wheel steering. For a second order model with zero trail ($c = 0$), the transfer function from steer angle δ to roll angle φ is as follows (it is identical to the transfer function of front-wheel steering model except in the sign of the velocity)

$$G_{\varphi\delta}(s) = \frac{aV}{bh}\,\frac{s - \frac{V}{a}}{s^2 - \frac{g}{h}}$$

Pole-Zero map of this system is plotted in the figure below:

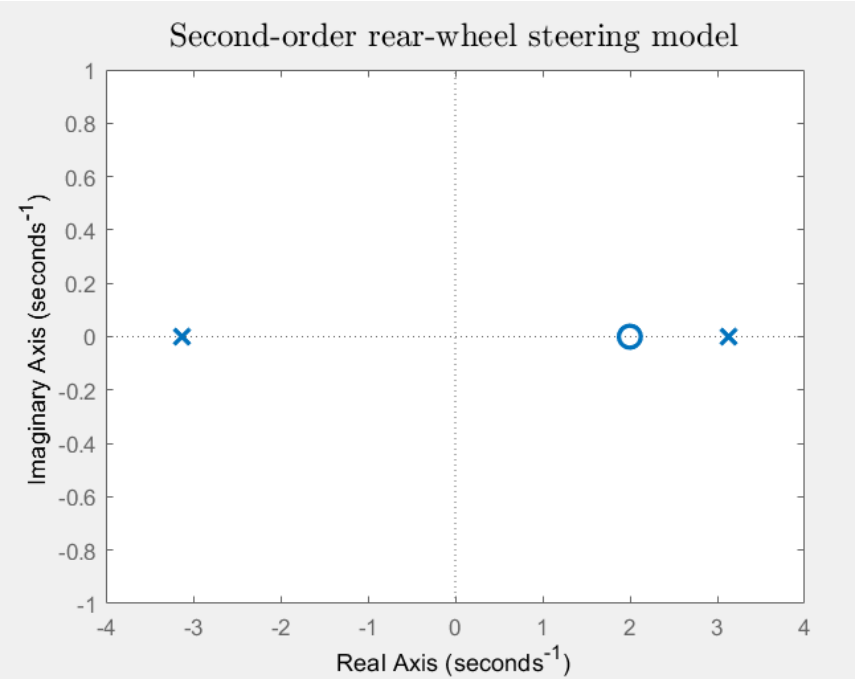

The open loop system has one pole and one zero in the right half plane which indicates the system instability. Attempting to stabilize the system using the same control law applied in front-wheel steering model, we obtain the following equation for tilt angle:

$$J\frac{d^2\varphi}{dt^2} - \frac{DVk_2}{b}\frac{d\varphi}{dt} + \left(\frac{mV^2hk_2}{b} - mgh\right)\varphi = 0$$

The characteristic equation of this differential equation is:

$$Js^2 + \frac{DVk_2}{b}s + \left(\frac{mV^2hk_2}{b} - mgh\right) = 0$$

Using approximations of J and D we find

$$mh^2s^2 + \frac{mahVk_2}{b}s + \left(\frac{mV^2hk_2}{b} - mgh\right) = 0$$

By the same reasoning as in first model, it can be shown that the system is unstable for all positive velocities and values of the feedback gain K_2. Moreover it can be shown that the system is unstable regardless of what controller law is used to control the system since there are fundamental problems in controlling a system with poles and zeros in the right-half plane.

In the figure below, root locus of the characteristic equation is drawn with respect to velocity and it verifies the system instability.

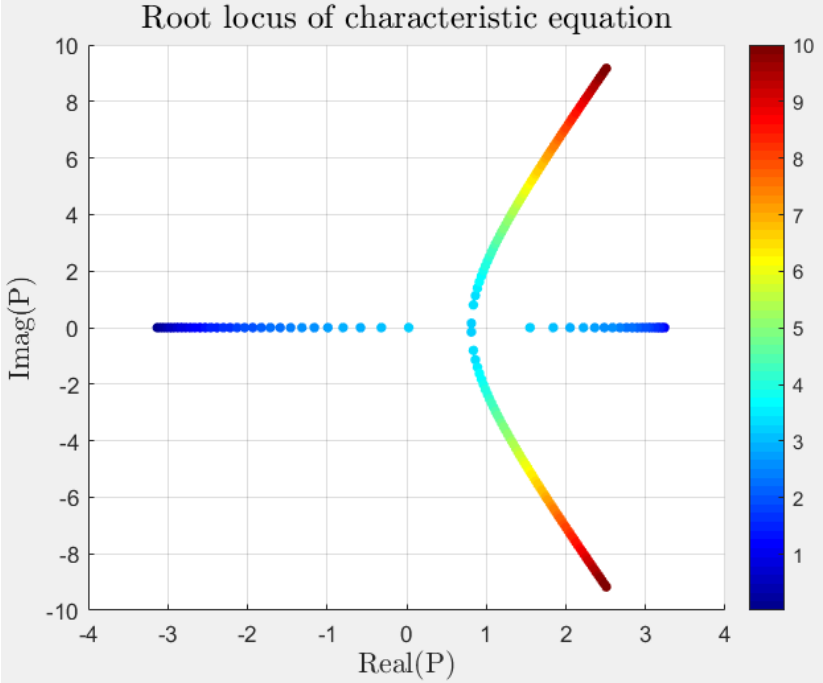

Roots of the characteristic equation of the closed-loop system

The color bar shows the velocity (dark blue dots correspond

to small velocities whereas dark red dots indicate higher velocities)

2.4) A Linear Fourth-Order Model

To extend second-order model, the static front fork model is replaced with dynamic model which yields the fourth-order model

$$M\begin{pmatrix}\ddot{\varphi}\\ \ddot{\delta}\end{pmatrix} + CV\begin{pmatrix}\dot{\varphi}\\ \dot{\delta}\end{pmatrix} + (K_0 + K_2V^2)\begin{pmatrix}\varphi\\ \delta\end{pmatrix} = \begin{pmatrix}0\\ T\end{pmatrix}$$

By taking the Laplace transform and solving for $\begin{pmatrix}\varphi\\ \delta\end{pmatrix}$ we obtain

$$\begin{pmatrix}\varphi\\ \delta\end{pmatrix} = (Ms^2 + CVs + K_0 + K_2V^2)^{-1}\begin{pmatrix}0\\ T\end{pmatrix}$$

$$\begin{pmatrix}\varphi\\ \delta\end{pmatrix} = \begin{pmatrix}G_{11} & G_{12}\\ G_{21} & G_{22}\end{pmatrix}\begin{pmatrix}0\\ T\end{pmatrix}$$

$$\varphi = G_{12}T\,,\delta = G_{22}T$$

Then the transfer functions from torque T to roll angle φ is

$$G_{\varphi T}(s) = G_{12}(s)$$

The elements of the matrices depend on the geometry and mass distribution of the bicycle. For the parameters given in the question, following values are derived using multibody programs:

$$M = \begin{pmatrix} 96.8\ (6.00) & -3.57(-0.472) \\ -3.57\ (-0.472) & 0.258\ (0.152) \end{pmatrix},$$
$$C = \begin{pmatrix} 0 & -50.8\ (-5.84) \\ 0.436\ (0.436) & 2.20\ (0.666) \end{pmatrix},$$
$$K_0 = \begin{pmatrix} -901.0\ (-91.72) & 35.17\ (7.51) \\ 35.17\ (7.51) & -12.03\ (-2.57) \end{pmatrix},$$
$$K_2 = \begin{pmatrix} 0 & -87.06\ (-9.54) \\ 0 & 3.50\ (0.848) \end{pmatrix}.$$

The values in the parentheses are for the bicycle without a rider.

To access animated graph for this model, run the code in section7 of the attached “Main.m” file.

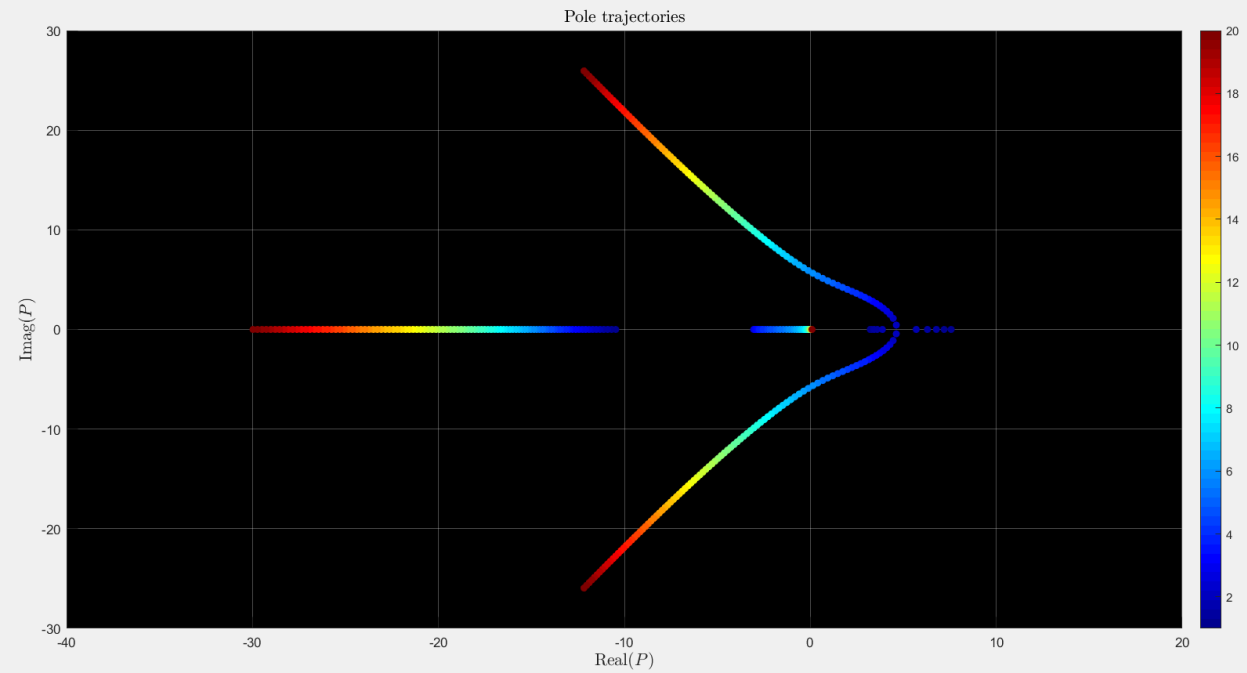

Root locus for the fourth-order model with respect to velocity

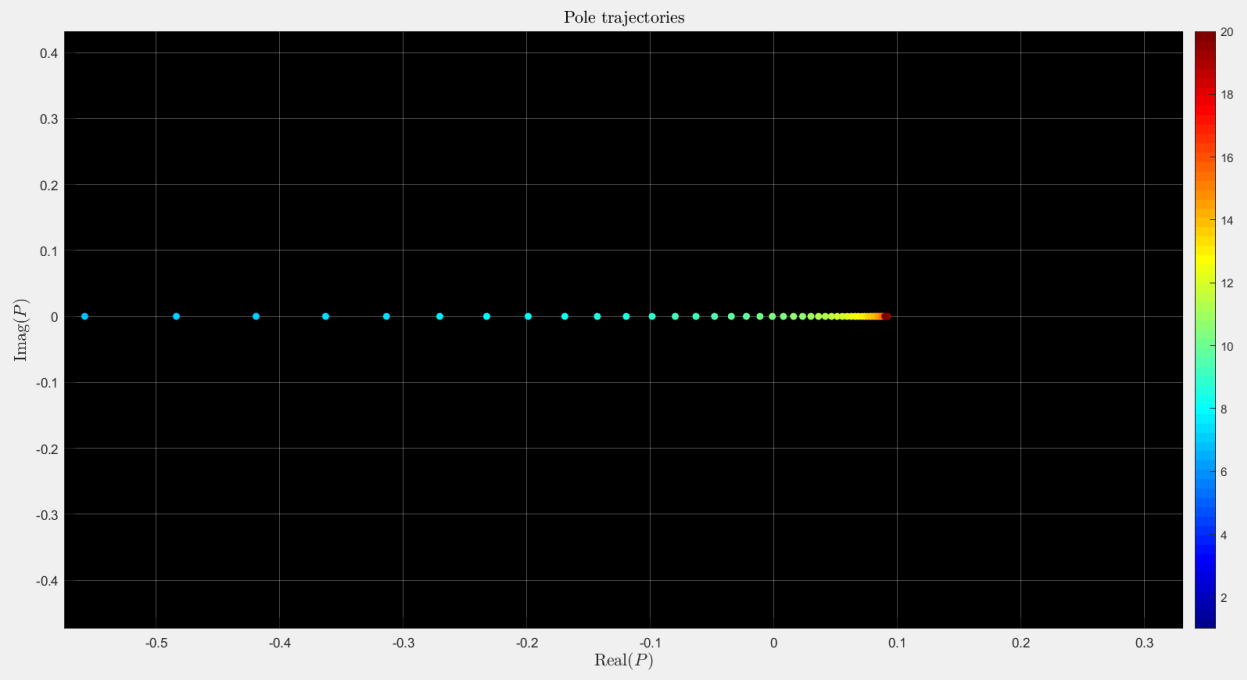

Zoomed version of the above figure which shows that the system becomes unstable for high velocities

According to the figures above, the system is initially unstable for low velocities. By increasing velocity, the system becomes stable but if velocity goes above a certain value, as the second figure suggests, one of the poles moves to the right-half plane and the system becomes unstable again. This is quite intuitive because it is difficult to control the bicycle in very low and very high velocities. Approximate velocity range for which the bicycle is stable is $6\ m/s \leq V \leq 10\ m/s$.

3) Maneuvering

In this scenario, the main problem is to determine how the toque on the handlebars influences the path of bicycle. Using the coordinate system introduced in the article and some simplifications, the transfer function from steer angle δ to path deviation η is

$$G_{\eta\delta}(s) = \frac{V^2}{bs^2}$$

Combining $G_{\eta\delta}(s)$ with $G_{\delta T}(s)$ for each model, gives the transfer function from torque T to η

$$G_{\eta T}(s) = G_{\eta\delta}(s) \cdot G_{\delta T}(s)$$

3.1) Simple Second-Order Model with a Front Fork

The transfer function from torque T to steer angle δ for this model is

$$G_{\delta T}(s) = \frac{K_1(V)}{1 + K_2(V)G_{\varphi\delta}(s)}$$

where $K_1(V)$ and $K_2(V)$ are defined in stabilization section.

$$G_{\eta T}(s) = G_{\eta\delta}(s) \cdot G_{\delta T}(s)$$

$$G_{\eta T}(s) = \frac{K_1(V)}{1 + K_2(V)G_{\varphi\delta}(s)} \cdot \frac{V^2}{bs^2}$$

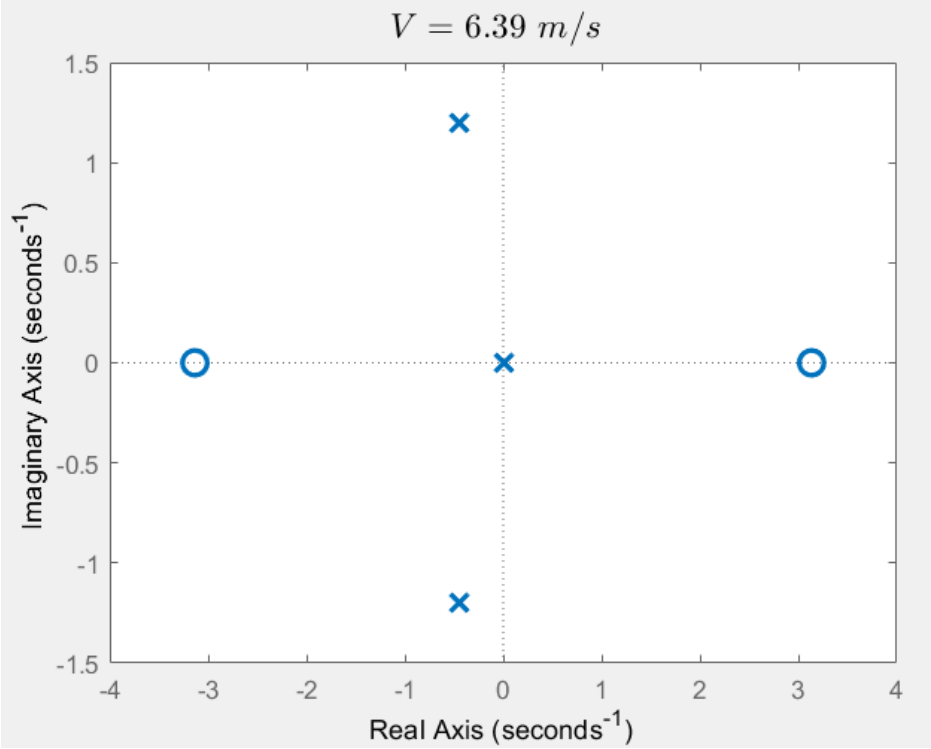

Pole-Zero map of $G_{\eta T}(s)$

the system is non-minimum phase since it has one zero in the right-half plane

To investigate maneuverability of this bicycle model, a positive torque-step ($T(t) = u(t)$) is applied to handlebars and the bicycle response is depicted in the following figures. Also notice that the velocity is chosen above critical velocity to make sure that the system is stable.

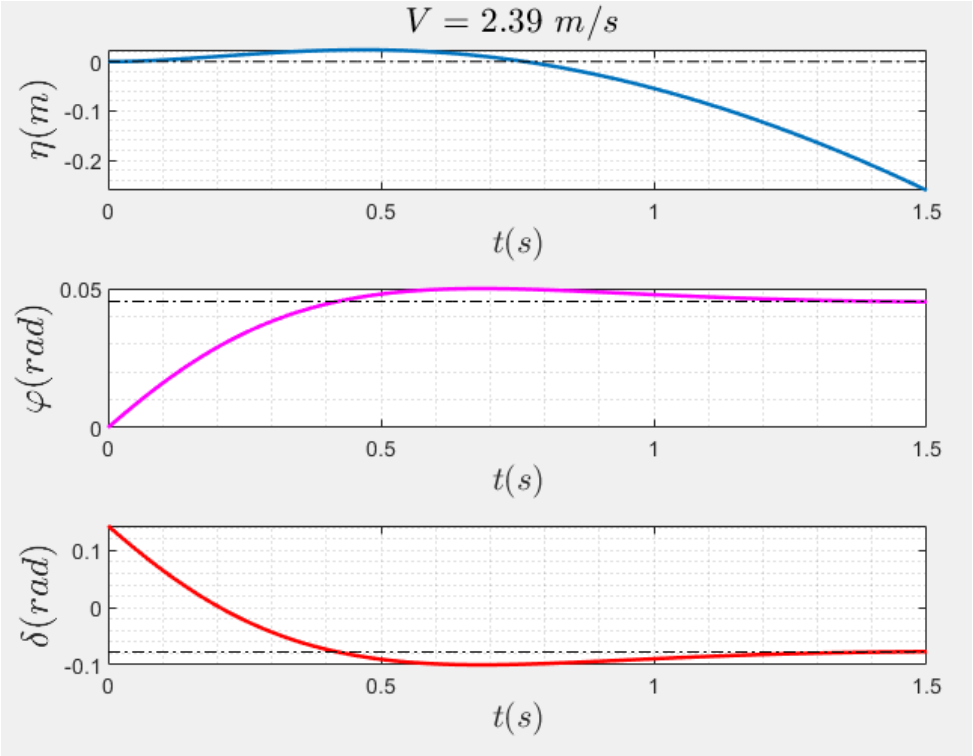

Notice that the path deviation η is initially positive but later becomes negative. This inverse response behavior is due to the right-half-plane zero and the physical reasoning can be found in page 33-34 of the reference article. In the above figure, the tilt angle settles to $\varphi = 2.6°$ and the steady-state value for steer angle is $\delta = -4.47°$.

3.2) Bicycle with Rear-Wheel Steering

Since this model is unstable for all positive velocities, no one can ride it and it doesn't make a sense to investigate maneuverability.

3.3) A Linear Fourth-Order Model

As discussed in section 2.4, transfer functions of this model can be obtained from the differential equation defining the model as follows:

$$\begin{pmatrix}\varphi\\ \delta\end{pmatrix} = (Ms^2 + CVs + K_0 + K_2V^2)^{-1}\begin{pmatrix}0\\ T\end{pmatrix}$$

$$\begin{pmatrix}\varphi\\ \delta\end{pmatrix} = \begin{pmatrix}G_{11} & G_{12}\\ G_{21} & G_{22}\end{pmatrix}\begin{pmatrix}0\\ T\end{pmatrix}$$

$$\varphi = G_{12}T\,,\ \delta = G_{22}T$$

$$G_{\varphi T}(s) = G_{12}(s)$$

$$G_{\delta T}(s) = G_{22}(s)$$

where M, C, K_0, K_2 are 2-by-2 matrices obtained using multibody software and by having $G_{\eta\delta}(s)$, we can easily obtain the transfer function from torque T to path deviation η:

$$G_{\eta T}(s) = G_{\eta\delta}(s)\cdot G_{\delta T}(s) = \frac{V^2}{bs^2}\cdot G_{22}(s)$$

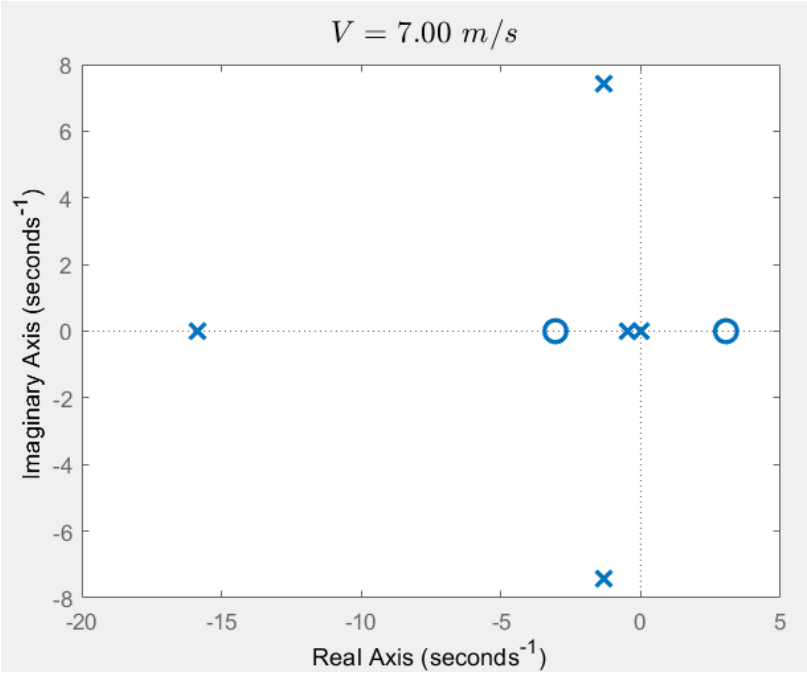

Pole-Zero map of $G_{\eta T}(s)$

the system is non-minimum phase since it has one zero in the right-half plane

The figure below shows system response when a positive torque-step is applied to handlebars. The velocity is chosen such that the system is stable. Again, the system exhibits inverse behavior which is clearly visible in the first sub-plot. The tilt angle settles to $\varphi = 47°$ whereas the steer angle settles $\delta = -10.10°$.

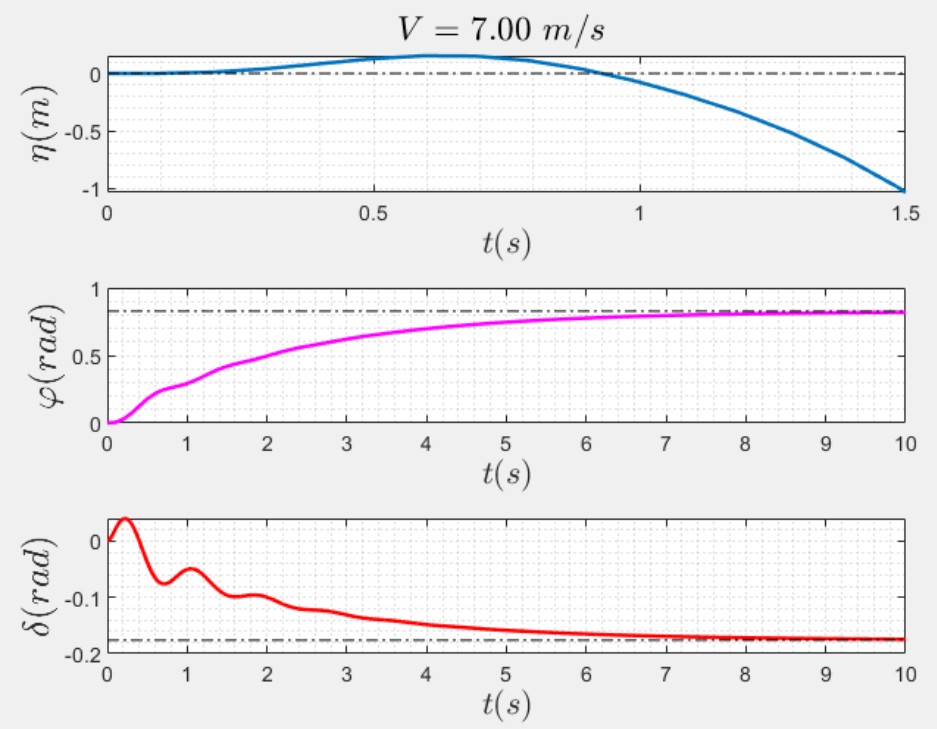

4) Effects of Rider Lean

To take rider lean into account, we consider the rider as composed of two rigid pieces, the lower body and the upper body, where the upper body can be rotated as illustrated in the figure below.

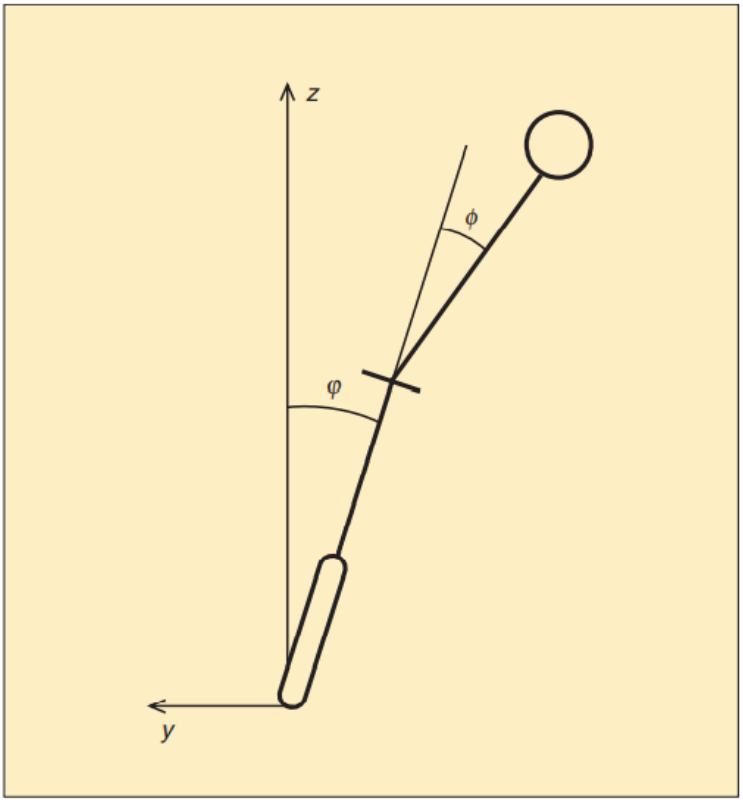

Figure 6. *Rear view of the bicycle with a leaning rider. The bicycle roll angle is φ, while the rider lean relative to the bicycle is ϕ.*

Writing momentum balance and combining it with the static model of the front fork, gives a model with a leaning rider:

$$J\frac{d^2\varphi}{dt^2}+\frac{DVk_2(V)}{b}\frac{d\varphi}{dt}+\left(\frac{mV^2hk_2(V)}{b}-mgh\right)\varphi=\frac{DVk_1(V)}{b}\frac{dT}{dt}+\frac{mV^2k_1(V)}{b}T-J_r\frac{d^2\phi}{dt^2}+m_rgh_r\phi$$

In the equation above, J_r is the moment of inertia of the upper body with respect to the x axis, m_r is the mass of the upper body, and h_r is the distance from the center of mass of the upper body to its turning axis. $k_1(V)$ and $k_2(V)$ are defined as in section 2.2.

The difficulties associated with the right-half plane zero can be avoided because in this case the system has two inputs; namely steering and leaning. In general, difficulties with right-half plane zeros can be alleviated by adding either more sensors or actuators.

To see effects of rider lean, we consider the case that rider does not apply any torque to the handlebars and controls the bike just by leaning. The terms associated with T then disappears and we are left with the following transfer function from lean angle ϕ to the roll angle φ

$$G_{\varphi\phi}(s) = \frac{m_r g h_r - J_r s^2}{Js^2 + \frac{DVk_2(V)}{b}s + \frac{mV^2 h k_2(V)}{b} - mgh}$$

Values of J_r and m_r can be obtained from table1 of the article as follows

Table 1. Basic bicycle parameters. This table gives the mass, inertia tensor, and geometry for a standard bicycle with a rider. The values in parentheses are for a bicycle without a rider.

	Rear Frame	Front Frame	Rear Wheel	Front Wheel
Mass m [kg]	87 (12)	2	1.5	1.5
Center of Mass				
x[m]	0.492 (0.439)	0.866	0	b
z[m]	1.028 (0.579)	0.676	R_{rw}	R_{fw}
Inertia Tensor				
J_{xx} [kg-m^2]	3.28 (0.476)	0.08	0.07	0.07
J_{xz} [kg-m^2]	−0.603 (−0.274)	0.02	0	0
J_{yy} [kg-m^2]	3.880 (1.033)	0.07	0.14	0.14
J_{zz} [kg-m^2]	0.566 (0.527)	0.02	J_{xx}	J_{xx}

$$m_r = 87 - 12 = 75\ kg$$

$$J_r = 3.28 - 0.476 = 2.804\ kg.m^2$$

We also assume that $h_r = 0.3\ m$ which seems reasonable for an adult.

In the following figure, pole locations are depicted for $0 < V < 2V_c$

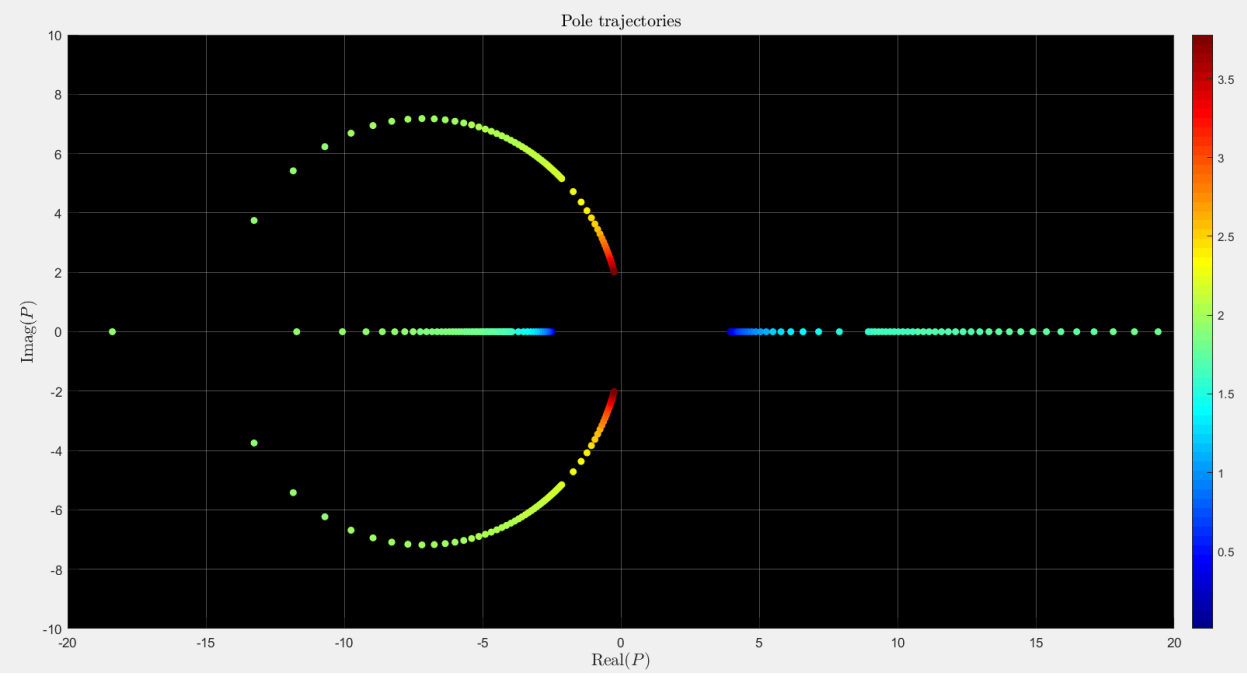

As expected, the system is unstable for low velocities but it becomes stable when the velocity exceeds a certain threshold. The threshold is about $1.9\ m/s$ for this configuration.

Next we investigate the system response to a step change in lean angle ϕ.

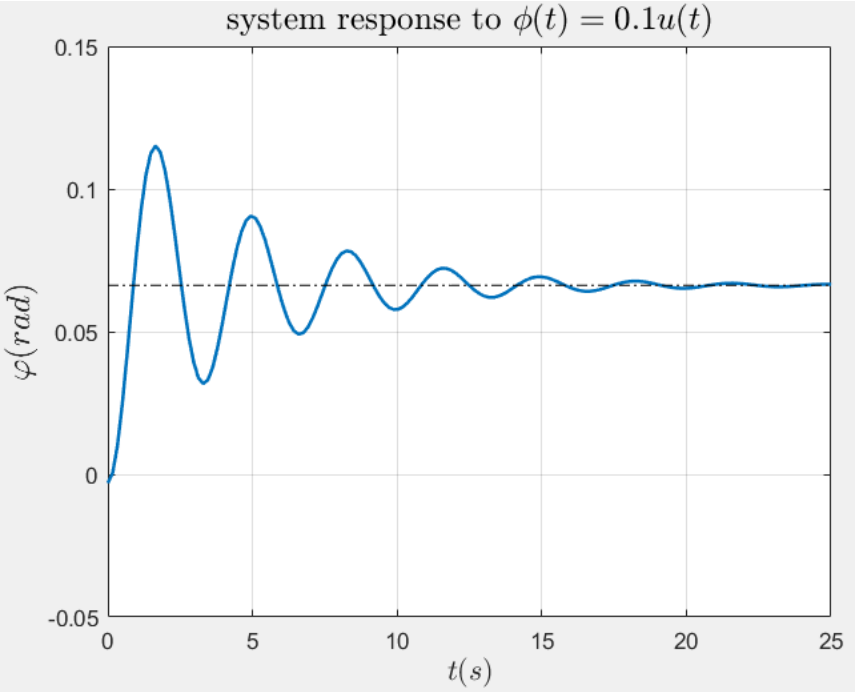

It is observed that the system oscillates and finally reaches equilibrium at $\varphi = 3.80°$.

5) Non-Minimum Phase Steering Behavior of bicycles

The picture on the right shows counter steering behavior of bicycles. To better understand this phenomenon, visualize a motorcycle driven along a straight path and assume that a car suddenly appears from the right. The intuitive reaction is to steer left, away from the car. Due to non-minimum phase nature of bikes, motorcycle initially does so but ultimately steers into the car. Significant number of motorcycle accidents are caused by novice riders who are not aware of this phenomenon. In this situation, the best thing to do is to simultaneously lean and counter steer.

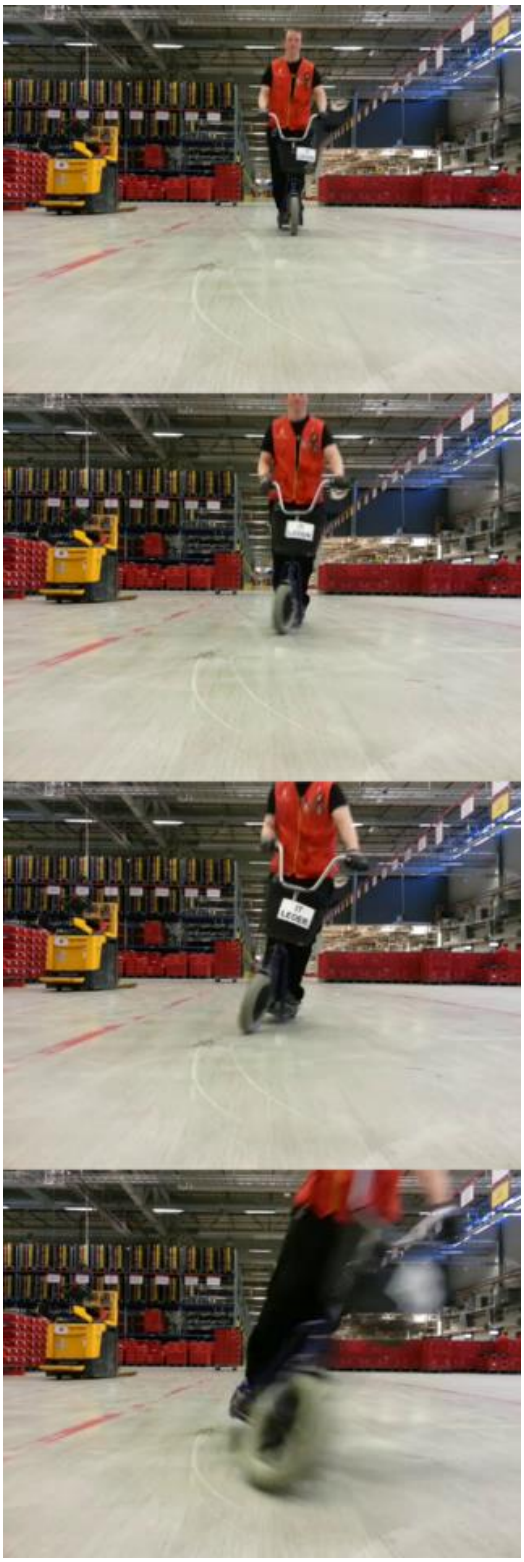

As indicated in section3, leaning alone is sufficient to change lane, but the dynamics of leaning alone are not fast enough to prevent accident in a such condition.

This type of behavior is typical for non-minimum phase systems. However, problems caused by right-half plane zeros can be alleviated by using more sensors. For example, using tilt and yaw rate sensors help to eliminate problems caused by right-half plane zero. It is interesting to note that skilled riders use steer torque, lean angle and variations in forward speed to eliminate right-half plane zero and get the desired behavior!